Positioning Impacts from Imbalanced Atmospheric GPS Network Errors

Yong Won Ahn, Don Kim and Peter Dare

Geodetic Research Laboratory, Department of Geodesy and Geomatics Engineering, University of New Brunswick, Fredericton, New Brunswick, Canada

BIOGRAPHY

Yong Won Ahn holds an M.Sc. from the Department of Geomatics Engineering at the University of Calgary awarded in 2005. He is currently a Ph.D candidate in the Department of Geodesy and Geomatics Engineering at the University of New Brunswick (UNB). His current research focuses on the tropospheric anomaly effect and the development of the enhanced network-based RTK system.

Don Kim is a senior research associate in the Department of Geodesy and Geomatics Engineering at UNB. He has a bachelor's degree in urban engineering, and an M.Sc.E. and Ph.D. in geomatics from Seoul National University. He has been involved in GPS research since 1991 and active in the development of ultrahigh-performance RTK systems. He received the Dr. Samuel M. Burka Award in 2003 from the Institute of Navigation.

Peter Dare is the Chair of the Department of Geodesy and Geomatics Engineering at UNB. He obtained a B.Sc. (Hons) in Land Surveying Sciences from North East London Polytechnic in 1980, an M.A.Sc. in Civil Engineering from the University of Toronto in 1983 and a Ph.D. in geodesy from the University of East London in 1996. He joined UNB in 2000 and became the Chair of the Department in 2002. He was elected a Fellow of the Royal Institution of Chartered Surveyors (RICS) in 2000.

ABSTRACT

For dual-frequency GPS observables, one of the largest error sources affecting high-precision positioning solutions arises from the unmodelled troposphere. In normal tropospheric cases, it is difficult to evaluate its positioning impacts as the estimated parameters may be obscured by other error sources. In this paper, we have extensively analyzed GPS network data from one of the most inhomogeneous atmospheric cases. We have examined the positioning impacts due to additional tropspheric gradient parameter estimation. In total, a data set from 18 GPS stations for 9 days from the Korea peninsula has been collected and processed during the passage of typhoon RUSA in 2002. Based on the estimated tropospheric delays from the GPS observables, the precipitable water vapor (PW) has been calculated in order for it to be evaluated and compared with those from independent observables (radiosonde and real precipitation records). GPS-derived PW values (with the inclusion of the gradients) demonstrate that they are correlated with the time series of radiosondes and actual precipitation. In this imbalanced network case, we investigated the possible positioning improvement including the gradient parameters in the processing. Unlike when under normal tropospheric conditions, the additional gradient parameter estimation can greatly reduce the instability of a coordinate solution. In addition, we observed that this could be more important for a station which experienced more inhomogeneity from the troposphere.

INTRODUCTION

The received Global Positioning System (GPS) signal experiences many different error sources, but most of them can be well modelled or be well minimized. This is true especially in relative GPS positioning due to temporal and spatial correlation of the errors. Unlike the ionospheric errors and orbital errors, which can be reduced to sufficiently low manageable levels, errors in the tropospheric delay, which mostly contribute to errors in the height component of the station's coordinate estimates, are known to be one of the largest limiting factors for high accuracy GPS positioning, at the current time. Typically, the troposphere error equals 2.5 m in the zenith direction. It can be separated into two components, dry and wet component. The dry component which consists of 90% of total delay is stable and well predictable, whereas the wet component is highly variable. Assuming hydrostatic equilibrium, the dry component is well predicted whenever the surface pressure is known. Then the estimated dry component can be subtracted from the total delay to get the wet component. The wet component varies from a few mm level at the poles to up to 40 mm in the zenith direction in the tropics, and changes significantly in the direction of a weather front. As the highly variable tropospheric water vapor content makes the troposphere more difficult to model, problems exist for high accuracy geodetic applications. Standard troposphere mitigation approaches assume azimuthal symmetry as the tropospheric delay is assumed to vary only with elevation angle. The asymmetries in the tropospheric refraction are important at low elevations which should be estimated as well as the common zenith delays. This is especially true when a typhoon is nearby, or other extreme localized weather conditions, causing the atmosphere to be extremely inhomogeneous resulting in degradation of GPS positioning results. Similar to the ionospheric scintillation effects, severe tropospheric effects can also result in fading phase and signal strength such that the GPS receiver can not track the satellite signals. In addition to other degrading effects on a GPS network (such as the increase noise of a receiver due to thermal noise, cable, or environment factors [Langley, 1997]), these atmospheric effects severely affect the entire network solution as well. These imbalanced network errors can be transferred to the other network solutions or rover solutions. Even for a short baseline, imbalanced atmospheric errors are shown to have a severe impact on rover positioning solutions, resulting in a worsening of the quality of the positioning solutions [Ahn *et al.*, 2006; Lawrence *et al.*, 2006; Zhang and Bartone, 2006; and Huang and van Graas, 2006].

MOTIVATION

Imbalanced network errors can degrade the entire positioning performance. Such an imbalanced atmospheric phenomenon described in the above section has been observed in many different networks around the world. These include severe sand or dust storms, ionospheric scintillation effects, localized or regional tropospheric anomaly effects, etc. [Comparetto, 1993]. Occasionally, these phenomena are observed when a strong tropospheric anomaly exists within a network. This can adversely affect RTK rover positioning solutions as well as making the entire network solution corrupt. One such condition has been observed on a number of GPS permanent stations in Korea when a severe typhoon passed through the nation from 31st August to 1st Sepember 2002. At the peak of the precipitation on 31st August, receivers could not track the signals due to the lowered signal to noise ratio (SNR). Fading of the signals is caused by several factors such multipath, cables, bad line of sight due to the obscured Fresnel zone, or weather conditions. Under severe tropospheric conditions, the standard mitigation approach based on modeled or empirical mitigation is limited. The unmodeled errors will adversely affect the rover positioning solution as well as make the entire network solutions corrupt. Our research focus is to evaluate the possible positioning impacts from severe tropospheric inhomogeneous conditions through the inclusion of tropospheric gradient parameters in the processing.

METHODOLOGY

The neutral atmosphere is comprised of the actual troposphere, the tropopause and the stratosphere. The tropospheric delay of GPS signals depends on the index of refraction n along the signal path through the neutral atmosphere. The geometrical distance is different from the actual path due to different path delays in the troposphere and a vacuum. Total (or neutral) slant path delay is given by [Schuler, 2001]

$$\delta\rho_{trp} = \int_{path} n(s)ds - \int_{vac} ds = \int_{path} (n(s)-1)ds + \text{bending}. \quad (1)$$

For elevation angles above 20 degrees, the bending effect is less than 3 mm. However, for 5-degree elevation angles, the effect can be as larger as 17 cm [Skone, 2003]. This total delay can be divided into a hydrostatic (dry) component $\delta\rho_h$ and a non-hydrostatic (wet) component $\delta\rho_w$ as:

$$\delta\rho_{trp} = \delta\rho_h + \delta\rho_w. \quad (2)$$

In Eq. (1), the index of the refractivity (that is, the ratio of the speed of the propagation of electromagnetic wave in vacuum to the speed of the propagation of the medium) can be expressed in term of the refractivity, $\mathrm{N} = 10^6(n-1)$. The refractivity of humid air in a frequency band between 100 MHz and 20 GHz is given by Thayer [1974] as:

$$N = k_1 \frac{p_d}{T} Z_d^{-1} + k_2 \frac{e}{T} Z_w^{-1} + k_3 \frac{e}{T^2} Z_w^{-1}, \quad (3)$$

where

p_d : partial pressure of dry air (mbar), $p_d = p - e$ with p being the total pressure,

e : partial pressure of water vapor (mbar),

T : temperature ($^{\mathrm{o}}$K),

k_1, k_2, k_3 : refraction constants ($^{\mathrm{o}}$K /mbar, $^{\mathrm{o}}$K /mbar, $^{\mathrm{o}}$K/mbar^2),

Z_d^{-1}, Z_w^{-1} : inverse compressibility factors for dry and wet air which are empirical factors.

The first term in Eq. (3) is the hydrostatic component of the tropospheric delay and represents the effect of the induced dipole moment of the dry component. The second term is related to the dipole moment of water vapor and the last term represents the dipole orientation effects of the permanent dipole moment of water vapor molecules. The last two terms in Eq. (3) constitute the wet component of the refractivity. The refraction constants k_1, k_2 and k_3 are determined empirically. The inverse compressibility accounts for the difference between ideal gas assumptions and non-ideal gas behavior. The inverse compressibility and the pressure of water vapor are given by [Schuler, 2001; Thayer, 1974]

$$
\begin{aligned}
Z_d^{-1} &= 1 + p_d \cdot \left(57.97 \cdot 10^{-8} \cdot \left(1 + \frac{0.52}{T}\right) - 9.4611 \cdot 10^{-4} \cdot \frac{T_c}{T^2}\right) \\
Z_w^{-1} &= 1 + 1650 \frac{e}{T^3} \cdot \left(1 - 0.01317 T_c + 1.75 \cdot 10^{-4} T_c^2 + 1.44 \cdot 10^{-6} T_c^3\right) \\
e &= \frac{H_{rh}}{100} e^{-37.2465 + 0.213166 T - 0.000256908 T^2},
\end{aligned}
\tag{4}
$$

where

T_c : temperature in ($^\circ C$),

T : temperature (^{o}K),

H_{rh} : relative humidity (%).

The inverse compressibility factors Z_d^{-1} and Z_w^{-1} are associated with dry and wet air, respectively. They are empirically determined and can be modeled as a function of pressure and temperature as shown in Eq. (4). To define the zenith delay, it is necessary to express the refractivity in Eq. (3) in terms of the hydrostatic and wet components. With the assumption of hydrostatic equilibrium, the following relationship can be made:

$$
\begin{aligned}
k_1 \frac{p_d}{T} Z_d^{-1} &= k_1 \frac{\rho_d R_d T Z_d}{T} Z_d^{-1} = k_1 \rho_d R_d \\
&= k_1 \frac{\rho_d R_o}{M_d} = k_1 \left(\frac{\rho R_o}{M_d} - \frac{e}{T} Z_w^{-1} \frac{M_w}{M_d} \right),
\end{aligned}
\tag{5}
$$

where

R_o : universal gas constant (J mol^{-1} ^{o}K^{-1}),

R_d : specific gas constant for dry air,

M_w : molar weight of wet air (kg kmol^{-1}),

M_d : molar weight of dry air (kg kmol^{-1}),

ρ_d : density of dry air (kg m^{-3}),

ρ : total density for dry and wet air (kg m^{-3}).

By substituting Eq. (5) into Eq. (3), the refractivity can be rewritten as:

$$
\begin{aligned}
N &= k_1 \left(\frac{\rho R_o}{M_d} - \frac{e}{T} Z_w^{-1} \frac{M_w}{M_d} \right) + k_2 \frac{e}{T} Z_w^{-1} + k_3 \frac{e}{T^2} Z_w^{-1} \\
&= k_1 \frac{\rho R_o}{M_d} + k_2' \frac{e}{T} Z_w^{-1} + k_3 \frac{e}{T^2} Z_w^{-1}
\end{aligned}
\tag{6}
$$

and

$$
k_2' = \left(k_2 - k_1 \frac{M_w}{M_d} \right),
\tag{7}
$$

where

$k_1 = 77.6 \pm 0.05(^{o}\mathrm{K/hPa})$,

$k_2 = 70.4 \pm 2.2(^{o}\mathrm{K/hPa})$,

$k_3 = (3.739 \pm 0.02) \times 10^5 (^{o}\mathrm{K}^2/\mathrm{hPa})$.

Eq. (6) is useful because it allows a strict separation between the hydrostatic and the wet components. The hydrostatic component, from Eq. (6), becomes

$$
N_d = k_1 \frac{\rho R_o}{M_d}
\tag{8}
$$

and the wet component becomes

$$
N_w = \left(k_2' \frac{e}{T} + k_3 \frac{e}{T^2} \right) Z_w^{-1}.
\tag{9}
$$

The zenith hydrostatic (ZHD) and wet delay (ZWD) can be defined as:

$$
ZHD = 10^{-6} \int_{h_s}^{\infty} N_d \, dh
\tag{10}
$$

$$
ZWD = 10^{-6} \int_{h_s}^{\infty} N_w \, dh,
\tag{11}
$$

where

h_s : surface height,

dh : differential increment in height.

Almost 90% of the total delay occurs in the hydrostatic component, which varies slowly with time. This hydrostatic delay can be easily modeled with the assumption of hydrostatic equilibrium to an accuracy at a millimetre level [Mendes and Langley, 1995]. Unlike the hydrostatic part, the wet part has strong spatial and temporal variations. The effects of wet delay to the range can reach 10-40 cm. The relative errors of empirical and theoretical models are of the order of 10%. Large residual errors in modeling can cause significant errors in high-precision GPS positioning applications. These variations can generate relative and absolute tropospheric errors. The error in the estimation of tropospheric corrections for one station with respect to another in a network can cause relative tropospheric errors. As a result, these errors are mostly propagated into a station's height error. To reduce or minimize these errors arising from poor modeling of the wet troposphere, one possibility is to model the tropospheric refraction using a purely independent data set without GPS observations. The other approach is to estimate the tropospheric parameters directly using the available GPS data.

As described previously, the ZWD using GPS data can be calculated from the relationship, ZWD = ZTD – ZHD, where ZTD represents the zenith total delay. The total delay can be estimated from GPS data. The hydrostatic component can be determined when the surface pressure, height, and latitude are known using the Saastamoinen hydrostatic delay model [Saastamoinen, 1972]. Eq. (8) can be rewritten using the mean gravity acceleration as:

$$N_d = k_1 \frac{\rho R_o}{M_d} = k_1 R_d \rho = -k_1 R_d \frac{1}{g_m} \frac{dp}{dH}. \tag{12}$$

Substituted Eq.(12) to the Eq. (10) gives

$$\begin{aligned} ZHD &= 10^{-6} \int_{H_s}^{\infty} N_d dH \\ &= -10^{-6} k_1 R_d \frac{1}{g_m} \int_{p_s}^{\infty} dp = -10^{-6} k_1 R_d \frac{p_o}{g_m}. \end{aligned} \tag{13}$$

where g_m is the weighted mean gravity acceleration. The weighted mean gravitational acceleration at the center of mass of the vertical atmospheric column directly above the station can be approximated by the Saastamoinen equation [Davis *et al*., 1985] as:

$$\begin{aligned} g_m &= 9.784 \cdot (1 - 0.00266 \cos 2\varphi - 0.00028 H) \\ &= 9.784 \cdot f(\varphi, H), \end{aligned} \tag{14}$$

where φ and H (km) are the latitude and height of the station, respectively. Therefore, the ZHD becomes:

$$ZHD = \frac{0.0022767 p_o}{1 - 0.00266 \cos 2\varphi - 0.00028 H}. \tag{15}$$

The troposphere can be expanded to further distinguish between the azimuthally symmetric delay and asymmetric parts [Schuler, 2001]. The asymmetric components can be determined using a horizontal tropospheric gradient model. One way to deal with this is a 'tilting' technique [Rothather *et al*., 1997; Meindl *et al*., 2004]. Since the direction of the tropospheric zenith may not be the same as that of the geometrical or ellipsoidal zenith, the tropospheric zenith angle is introduced as a parameter of the mapping functions. Then, the tropospheric delay can finally be given as:

$$\begin{aligned} \delta\rho_{trop,k} &= \delta\rho_{trop,ini,k} f_{ini}(z_k^i) + \delta\rho_k^h f(z_k^i) \\ &+ \delta\rho_k^n \frac{\partial f}{\partial z} \cos(\alpha_k^i) + \delta\rho_k^e \frac{\partial f}{\partial z} \sin(\alpha_k^i), \end{aligned} \tag{16}$$

where:

α_k^i, z_k^i : azimuth angle and zenith distance of the satellite,

$\delta\rho_k^h$: zenith delay parameter,

$\delta\rho_k^n$: gradient parameter in North-South direction,

$\delta\rho_k^e$: gradient parameter in East-West direction,

f : mapping function.

In Eq. (16), the third and fourth terms are the troposphere gradient parameters in north-south and east-west direction. So, these parameters are estimated together with the residual tropospheric delays in this study. Once the ZWD is estimated, the PW (precipitable water vapor) can be calculated using Schuler [2001]:

$$Q = \frac{ZWD}{PW} = 0.10200 + \frac{1708.08\left({}^{\circ}\mathrm{K}\right)}{T_m}, \tag{17}$$

$$T_m = 70.29\left({}^{\circ}\mathrm{K}\right) + 0.72 T_0 \left({}^{\circ}\mathrm{K}\right), \tag{18}$$

where

T_m : mean temperature of the atmosphere degrees in Kelvin,

T_0 : surface temperature degrees in Kelvin.

In order to retrieve the PW, the mean temperature is necessary. We used the empirical values of Bevis *et al.* [1992] in Eq. (18) as the mean value for the region was not available for analysis. Mendes *et al*. [2000] also evaluated the weighted mean temperature for the global application.

The derived PW is then compared with that of the observed radiosonde. Even if the radiosonde has a poor horizontal resolution compared to the water vapor radiometer in a clear sky, it still provides good vertical atmospheric reference parameters during severe weather conditions. The total amount of the PW can be defined by integral of $\rho_v(z)dz$, where ρ_v is the mass density of the water vapor at altitude z .

DATA DESCRIPTION & PROCESSING STRATEGY

To evaluate the potential improvement of positioning performance by including the residual tropospheric delays and gradients as parameters in data processing, we analyzed a severe weather event. Figure 1 illustrates a typhoon, RUSA, passing over the South Korea peninsular in summer 2002. The typhoon was one of the worst in Korean history as it took 184 lives and destroyed 9900 buildings with resulting damage estimated at a value at C$ 6.8 billion. The image in figure 1 is a GMS infrared satellite image. The data sets taken from 18 different permanent GPS stations in Korea from August 25 to September 3 are extensively analyzed for evaluating the positioning impact from the imbalanced network errors. The processing is based on double differences. To get the best possible absolute ZTDs, and to decorrelate the zenith delay and height component, one distant stations, TSKB in Japan, is incorporated into the data analysis.

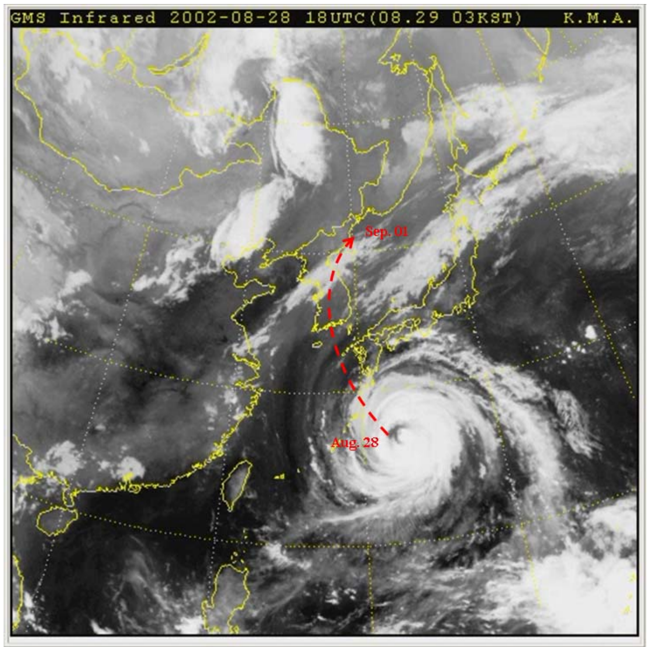

Figure 1. Infrared image taken by GMS at 18 UTC on 28 August 2002 [KMA, 2002].

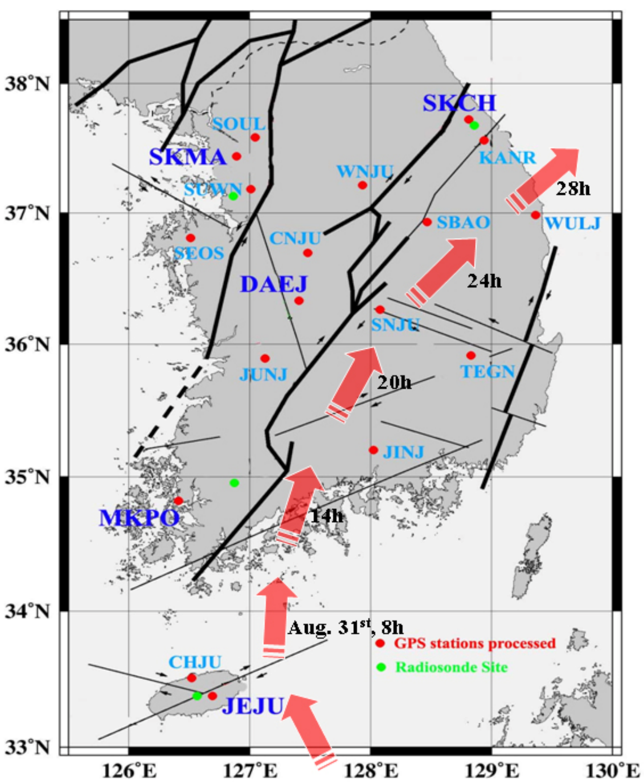

Figure 2. The track of the typhoon, RUSA, and the stations involved in the research.

Figure 2 illustrates the detailed track of the typhoon and approximate station coordinates used in this research. The time of the track is referenced to UTC. All of the data from the 18 GPS stations illustrated are extensively processed. Green dots in Figure 2 represent the sites for radiosondes which are processed for evaluating the calculated PW validation. The station coordinates are presented in Table 1.

Table 1. Station coordinates involved.

ID	Lat.(deg.)	Long.(deg.)	Hgt(m)
KANR	37.7667	128.867	57.0531
MKPO	34.8167	126.367	64.4074
SBAO	36.9333	128.45	1369.34
SKCH	38.25	128.55	46.0738
SEOS	36.7667	126.483	52.2683
SKMA	37.4833	126.917	61.7199
CHJU	33.5	126.517	50.3485
CNJU	36.6167	127.45	93.5029
DAEJ	36.3833	127.367	116.848
JEJU	33.2833	126.45	430.226
JINJ	35.1667	128.033	122.013
JUNJ	35.8333	127.133	77.1584
SNJU	36.3667	128.133	111.587
SOUL	37.6167	127.067	59.1093
SUWN	37.2667	127.05	83.8157
TEGN	35.9	128.8	106.386
WNJU	37.3333	127.933	180.215
WULJ	36.9833	129.4	80.7422

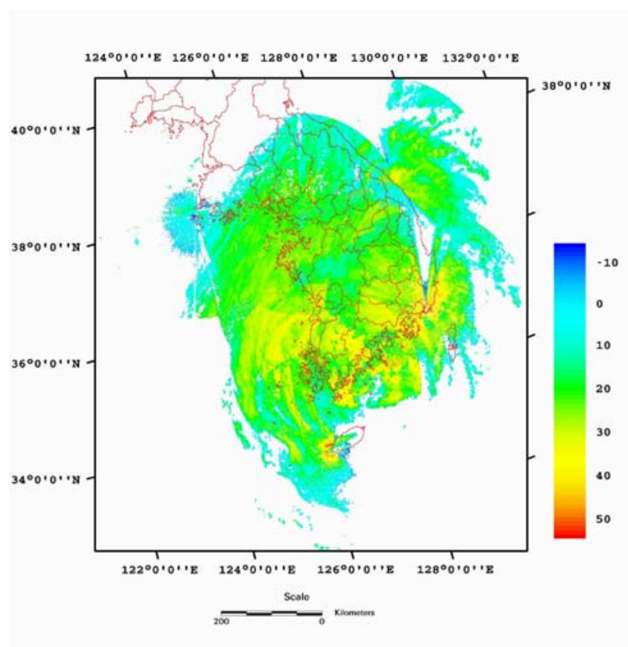

Figure 3. Composite reflectivity (dBZ) at 06:00 hrs on August 31, 2002 UTC [Tachikawa *et al*., 2003].

In addition to the GMS image, radar observations are included from Cheju (DWSR90C), Backryung, Dong-Hae

(DWSR90), Jindo, Kunsan (DWSR90C), Mt. Kwana (DWSR -8) and Pusan (DWSR90C) as shown in Figure 3. This figure shows the reflectivity composite image at 15.00 hrs on August 31, 2002 local time [Tachikawa *et al.*, 2003]. All of the data sets are recorded based on Trimble's SSI GPS receivers with a data rate of 30 seconds.

For processing the GPS data, Bernese software was used. Once all of the station networks were formed and cycle slips were correctly detected and repaired, the L1 and L2 ambiguities were resolved using a stochastic ionosphere approach (namely, the quasi-ionosphere approach). After all possible ambiguities were resolved, these ambiguities were fixed to get the final positioning solutions. Subsequently, troposphere parameters were estimated. To evaluate and try to mitigate the imbalanced network error, a gradient model described earlier was set up as an additional parameter in the processing. During Bernese data processing, IGS final SP3 orbit products were used. The tropospheric estimation described earlier with elevation-dependent weighting was also used in the processing.

RESULTS

For the processing, the recorded pressure, temperature, and radiosonde data from the Korea Meteorological Administration (KMA) were used. Figure 4 represents the pressure curve recorded.

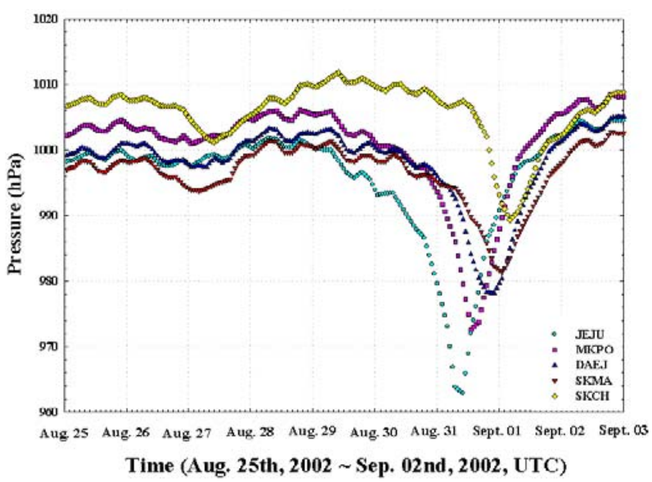

Figure 4. Pressure profiles when the typhoon was crossing the nation.

Based on the above pressure curve, the typhoon was crossing the nation during August 31^{st} and September 1st. From Figure 2, the track across Korea was from the south to the north. During the same period of time, torrential rain occurred.

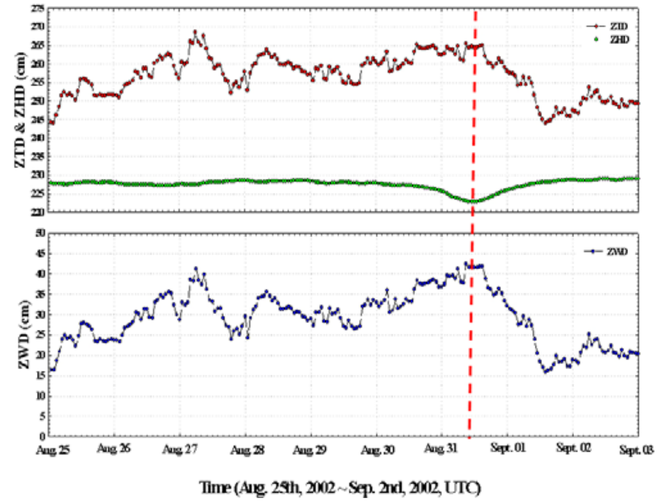

Figure 5. Zenith total, hydrostatic and wet delays at station DAEJ.

Figure 5 represents one example of the estimated ZTD using GPS data, and the ZHD based on the Saastamoinen model using surface pressure; this is for station DAEJ. The red dashed line is the time when the typhoon passed. The ZTD can be estimated from the GPS data and then subtracted from the ZHD to get the lower plot, the ZWD. The lower plot in Figure 5 clearly illustrates that the wet delay component has a peak value when the typhoon is nearby.

Tropospheric PW and Gradient Estimation

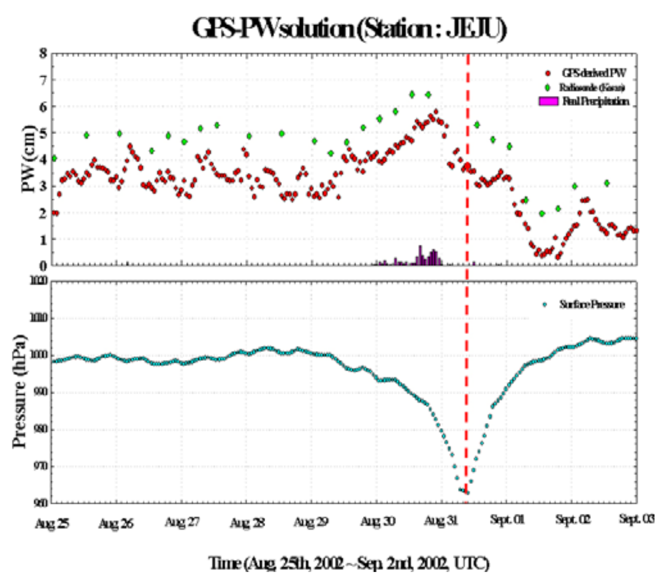

Figure 6. The zenith total, hydrostatic, and wet delays at station JEJU.

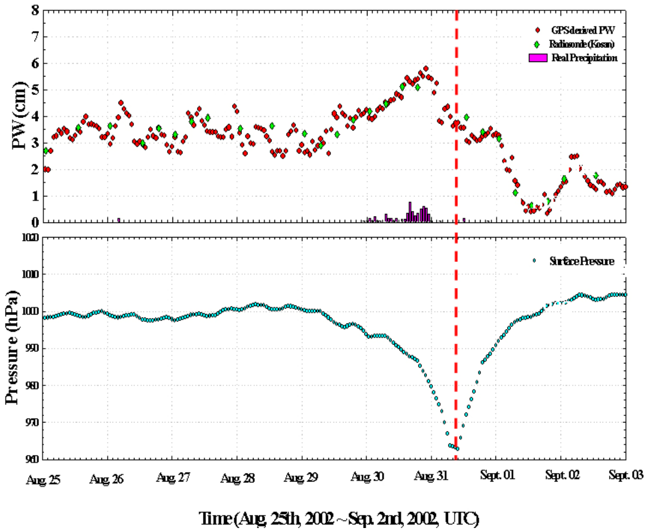

Figure 7. PW from GPS and radisonde, real precipitation, and pressure profile during the passage of a typhoon, RUSA, in summer 2002 at station JEJU.

Figure 6 is a sample plot of the estimated PW by GPS and radiosondes over 9 days. The pink bar is the actual precipitation water amount per hour recorded by the meteorological centre during that time. The bottom panel shows the pressure in hPa. As seen in the plots, both PW and the precipitation show strong correlation with the pressure. As most of the radiosonde stations are not at exactly the same location as the GPS station, differences can be seen. The height difference for radiosonde and GPS in this case is around 350 m and so the corresponding pressure and temperature need to be corrected. In this case, an exponential decay function for pressure and constant lapse rate for temperature for the atmosphere are applied for minimizing the height differences. After corrected, as is expected, those three values generally agree well.

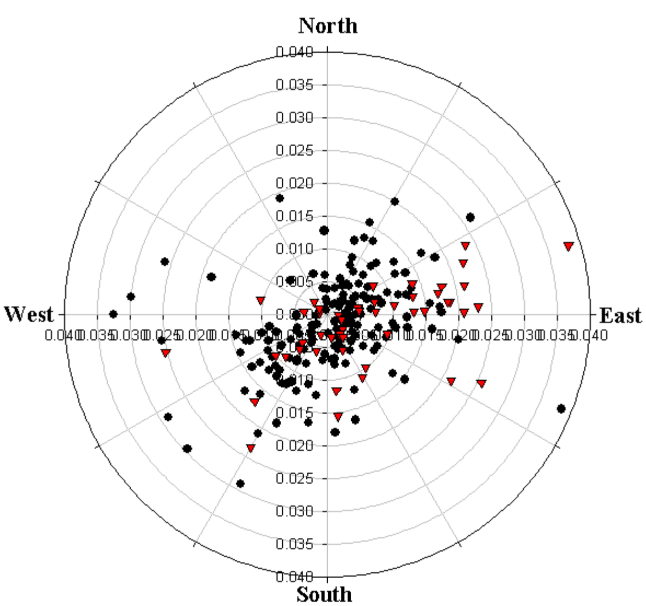

Figure 8. Horizontal gradients estimated for station JEJU.

As described earlier, the atmosphere is extremely inhomogeneous when the typhoon is close. We hourly estimated the gradient for the period from August 25th to September 2nd during the GPS processing and Figure 8 expresses those estimated total gradients. Black dots and red triangles represent the estimated gradient values. Specifically, the red triangles are the estimated gradients from August 31 to September 1 during the passage of the typhoon. As is shown, the red triangles are slightly biased in the south eastern direction which agrees with the location of the typhoon from the satellite image.

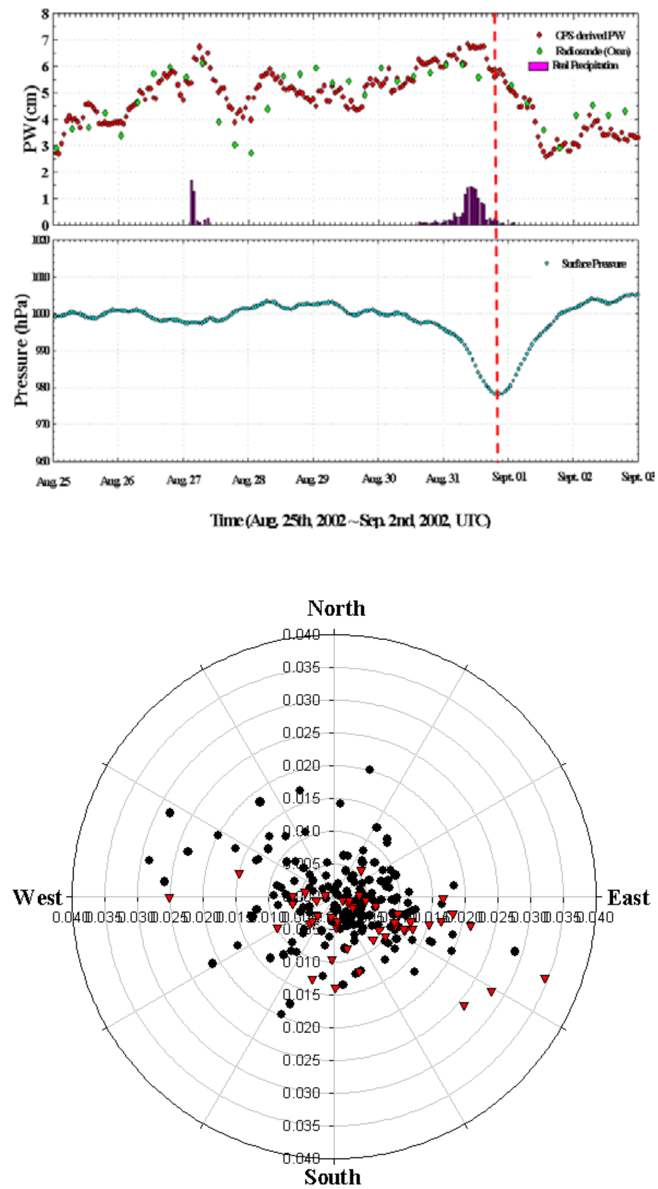

Figure 9. PW from GPS and radisonde, real precipitation, pressure profile (upper plot), and horizontal gradients estimated for DAEJ station (lower plot) during the passage of a typhoon, RUSA, in summer 2002.

Figure 9 represents the PW from GPS and radiosonde measurements, and the pressure profile for station DAEJ, near central part of the nation. The two PW values generally agree, but there are some differences. We believe that the difference is due to a difference in the location of the GPS receiver and radiosonde.

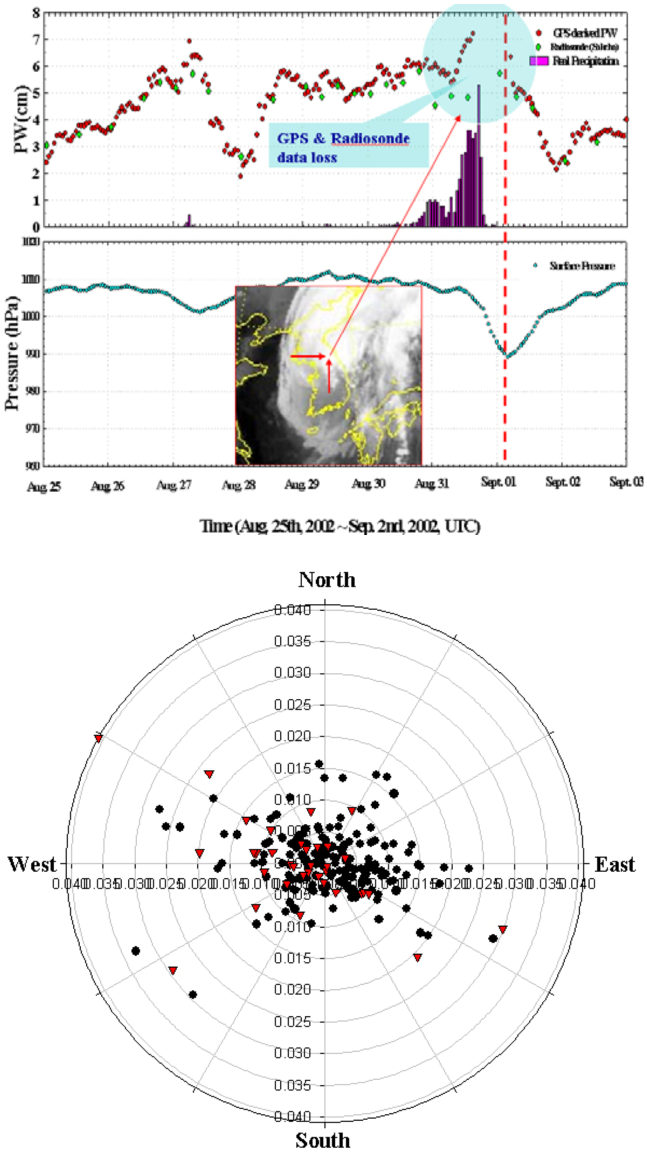

Figure 10. PW from GPS and radisonde, real precipitation, pressure profile (upper plot), and horizontal gradients (lower plot) for station SKCH.

Figure 10 shows the estimated PW values for station SKCH. This area was the one of the heaviest rainfall areas during the day. It can be validated based on the actual precipitation and the satellite image. The observed PW is high before and during the passage of the typhoon, and then decreases rapidly right after its passage. During the passage of the typhoon, some of the GPS and radiosonde data were missing and they are indicated by gaps in the plot. The red dashed line represents when the typhoon was close to the station; the estimated gradients are in the direction of N-W quadrant. These estimated gradients are also highly correlated with time with the weather image recorded.

Coordinate Differences with / without Horizontal Gradient Estimates.

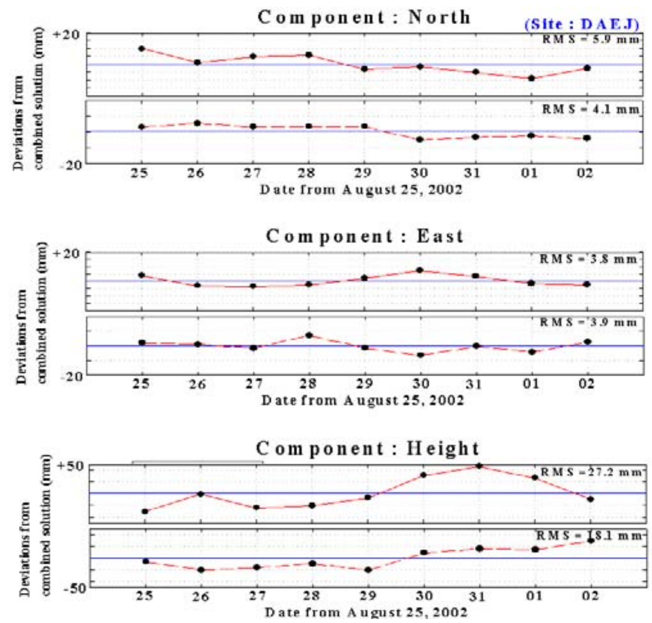

Figure 11. Coordinate differences for station DAEJ in north, east and height components. In each component, the upper plot is the coordinate delta without gradient estimates, and the low plot is that with the gradients.

By introducing the residual tropospheric delays and gradients as parameters in data processing, the daily repeatibilities of the coordinate solution are improved. This can be important when a local or regional anomaly exists. In this case, the theoretical or empirical tropospheric mitigation technique can be marginally efficient. The top panel of each coordinate component in Figure 11 shows the solutions estimated without horizontal gradients while the bottom panel shows the solutions using gradient estimates in the processing. As illustrated in the above figure, an improvement can be seen in each component. Noticeable is that the improvement of the height component was higher in terms of absolute value, than that of the horizontal component as the troposphere is correlated more with the height component. Please note that the y-scale is different in the height component.

Considering gradients in the processing is more important when the local troposphere is extremely inhomogeneous. Station SKCH experienced one of the heaviest downpours during the passage.

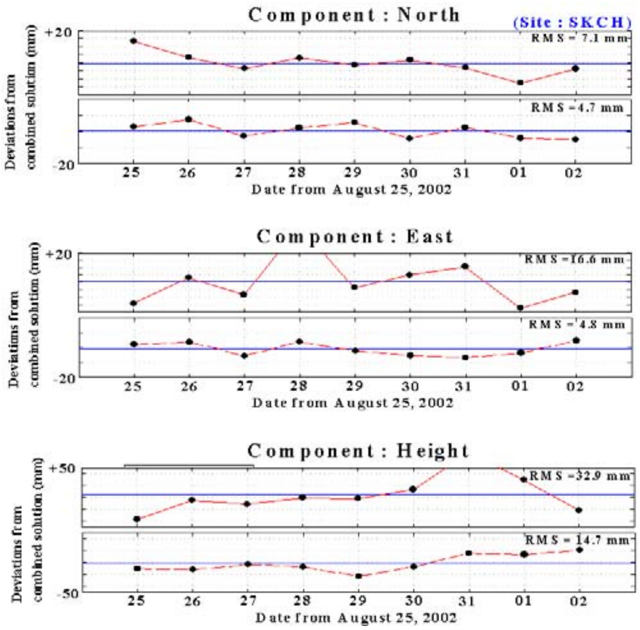

Figure 12. Coordinate differences for station SKCH in north, east and height component.

The coordinate improvement can be seen in Figure 12 and is higher than any other stations. Introducing the gradients can greatly improve the positioning solution when severe tropospheric events happen. Figure 12 shows the coordinate differences between the fixed coordinates which are from the combined solutions for a few months and the estimated solutions for each station. The positioning improvement in terms of RMS reaches 34% in the north, 72% in the east, and 55% in the height component. We found that the gradient estimation has a significant contribution on the stability of the internal precision of the coordinate solutions.

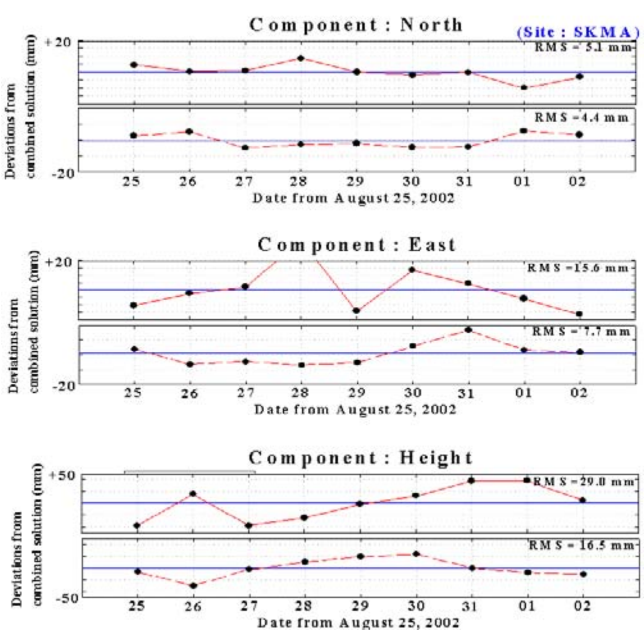

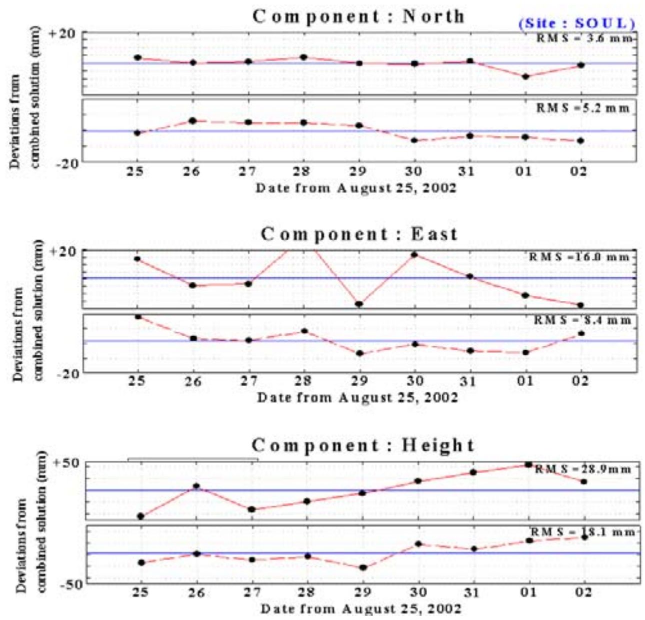

Figure 13. Coordinate differences for stations SKMA and SOUL in north, east and height components.

For short baselines with little height difference, the troposphere is usually strongly correlated at each receiver so that there is little benefit in using a sample tropospheric model. However, when a weather front is approaching, or a sudden atmospheric anomaly case occurs, this is no longer valid. In this case, introducing a more sophisticated mitigation model must be necessary. An example is included in Figure 13. The baseline length for SKMA and SOUL is around 20 km which can be regarded as short to medium range. The upper plot on each component in Figure 13 shows almost the same pattern for both stations before introducing the gradient parameter. After introducing the gradients (which provide more realistic models in this case) these two patterns are totally different while improving the coordinate solution.

Table 2 summarizes the improvement of all involved stations before and after the gradient estimation. Almost all of the stations present consistent improvement in the positioning solution. Even if we have a redundancy issue on adding additional parameters (especially in GPS RTK positioning), we conclude that the inclusion of the gradients is important for the short baseline case especially when there is strong imbalanced atmospheric network errors. The improvement could be more dramatic when more satellites are available.

Table 2. Summary of the positioning improvement for all 18 GPS stations.

	North(RMS, mm)			East(RMS,mm)			Height(RMS,mm)		
ID	Non-Gradient	Gradient	Improve-ment(%)	Non-Gradient	Gradient	Improve-ment(%)	Non-Gradient	Gradient	Improve-ment(%)
KANR	6.0	**3.9**	35	13.5	**3.1**	77	24.4	**12.6**	48
MKPO	5.5	**4.1**	25	8.5	**4.6**	46	28.2	**14.2**	50
SBAO	6.5	**4.4**	32	12.5	**4.2**	66	31.0	**16.1**	48
SKCH	7.1	**4.7**	34	16.9	**4.8**	72	32.9	**14.7**	55
SEOS	7.1	**4.7**	34	17.1	**4.9**	71	28.8	**18.7**	35
SKMA	5.1	**4.4**	14	15.6	**7.7**	51	29.0	**16.0**	45
CHJU	4.7	**2.2**	53	9.5	**3.8**	60	26.0	**20.0**	23
CNJU	5.2	**4.5**	13	8.6	**3.9**	55	26.7	**18.0**	33
DAEJ	5.9	**4.1**	31	3.8	**3.9**	-3	27.2	**18.1**	33
JEJU	4.1	**3.7**	10	9.1	**3.7**	59	18.8	**17.3**	8
JINJ	4.1	**3.9**	5	8.4	**3.9**	54	22.7	**16.7**	26
JUNJ	5.6	**4.5**	20	7.2	**3.9**	46	30.7	**17.6**	43
SNJU	5.5	**4.5**	18	13.5	**6.8**	50	27.2	**15.6**	43
SOUL	3.6	**5.2**	-44	16.0	**8.4**	48	28.9	**18.1**	37
SUWN	5.2	**4.5**	13	16.8	**7.6**	55	22.2	**17.0**	23
TEGN	5.5	**3.3**	40	14.2	**5.9**	58	28.0	**16.5**	41
WNJU	5.1	**3.4**	33	16.0	**5.6**	65	21.9	**15.2**	31
WULJ	5.5	**4.6**	16	13.4	**5.0**	63	30.3	**23.9**	21

CONCLUSIONS

In this paper, we demonstrated the positioning impacts from imbalanced atmospheric errors on a network. For this purpose, an extensive test was performed when typhoon RUSA crossed the Korea peninsula from 25 August to 3 September 2002. We analyzed 18 GPS stations and estimated the corresponding ZTDs including gradients using Bernese software. Then, they were transformed to the ZWD using the pressure and temperature values recorded by the Korea Meteorological Administration at each station. These retrieved ZWDs were then used to derive the PW values in order to examine those retrieved precipitable water values, and determine whether or not the patterns agreed well with those from radiosondes and actual recorded precipitation. From the result, the retrieved signature shows an expected trend that is correlated with the estimated ZWDs. Also, the estimated PW values from GPS and radiosondes generally agree and show the correlation with the actual precipitation recorded by the Korea Meteorological Administration.

For the purpose of investigating the possible positioning improvement under severe imbalanced atmospheric conditions, gradients were incorporated into the processing. In a small network with normal tropospheric conditions, the additional estimation of tropospheric parameter may make the positioning solution unstable. This is because the introduction of another parameter in the estimation process may weaken the solution even though it is beneficial in reducing a certain type of bias or error. However, a realistic estimation of a 'correct' parameter is much more important especially whenever it is almost impossible to interpret or mitigate the errors based on the theoretical and empirical models. We investigated the possible positioning improvements after introducing additional parameters in the processing during inhomogeneous atmospheric conditions. When not under the normal tropospheric conditions, the additional gradient estimation can greatly reduce the instability of a coordinate solution. Based on this research, we also conclude that this gradient estimation could be more important for a station which experiences inhomogenity in the troposphere.

FUTURE WORK

As the troposphere is a limiting factor for high precision positioning, an extensive analysis of the imbalanced anomaly cases is necessary. Unfortunately, it is almost impossible to record such data sets due to the logistics. As a result, a series of imbalanced tropospheric phenomenon on a network is limited and difficult to obtain from real networks. In this case, a simulation would be preferable for extensive analysis of those impacts. This simulation can be possible after performing quantitative analysis of all possible errors through real observables. With the errors estimated for each station involved, for example, Spirent STR4760 L1/L2/L2C hardware simulators can be used for generating artificial observables to further analyze the GPS positioning errors due to the imbalanced network errors. Simulations can be included in the user-generated troposphere, ionosphere, multipath, receiver's antenna attenuation patterns and satellite's antenna attenuation patterns etc. These parameters have been estimated or modeled during this research. Therefore, once the relevant simulation data is generated based on them, further investigation to mitigate those errors can be performed.

ACKNOWLEDGMENTS

The authors would like to acknowledge Natural Sciences and Engineering Research Council of Canada (NSERC), the Canada Foundation for Innovation (CFI) and the New Brunswick Innovation Foundation (NBIF) for support for the research. Some parts of the research reported in this paper were carried out under contract specifically for GNSS simulation system development for modeling environmental error. The support of the Korea Astronomy and Space Institute (KASI) is greatly acknowledged. The authors also thank the Astronomical Institute of University of Bern for the Bernese software, supported by the Royal Institution of Chartered Surveyors (RICS) Education Trust.

REFERENCES

Ahn, Y. W., D. Kim, and P. Dare (2006). "Local tropospheric anomaly effects on GPS RTK performance", Proceedings of ION GNSS 2006, Fort Worth, Texas, U.S.A, pp. 1925-1935

Bevis, M, S. Brusinger, T. A. Herring, C. Rocken, R. A. Anthes, and R. H. Ware (1992). "GPS meteorology : Remote sensing of atmospheric water vapor using the Global Positioning System", *Journal of Geophysical Research*, Vol, 97, No. D14, pp. 15787-15801.

Comparetto (1993). "The impact of dust and foliage on singal attenuation in the millimeter wave regime", *Journal of Space Communication,* Vol 11, no.1, pp.13-20.

Davis, J. L., T. A. Herring, I. I. Sharpiro, A. E. E. Rogers, and G. Elgerred (1985). "Geodesy by radio interferometry: Effects of atmospheric modeling errors on estimates of baseline length", *Radio Science*, Vol. 20, No. 6, pp. 1593-1607.

Huang, J. and F. van Graas (2006). "Comparison of tropospheric decorrelation errors in the presence of severe weather conditions in different areas and over different baseline lengths", Proceedings of ION GNSS 2006, Fort Worth, Texas, U.S.A, pp. 2769-2787

KMA (2002). Korea Meteorological Administration, http://www.kma.go.kr/ [accessed in September, 2002].

Langley R. B. (1997). "GPS Receiver System Noise", *GPS World*, pp. 40-45.

Lawrence D., R. B. Langley, D. Kim, F. Chan, and B. Pervan (2006). "Decorrelation of troposphere across short baseline", IEEE/ION PLANS 2006, San Diego, California, U.S.A, pp. 97-102

Meindl, M., S. Schaer, U. Hugentobler, and G. Beutler (2004). "Tropospheric gradient estimated at CODE: Results from global solutions", *Journal of Meteorological Society of Japan*, Vol. 82 (1B), pp. 331-338.

Mendes, V. B. and R. B. Langley (1995). "Zenith Wet Tropospheric Delay Determination Using Prediction Model: Accuracy Analysis", *Cartograpia e Cadastro*, Vol.2, pp. 41-47.

Mendes, V. B., G. Prates, L. Santos and R. B. Langley (2000). "An Evaluation of the Accuracy of Models for the Determination of the Weighted Mean Temperature of the Atmosphere", Proceedings of ION National Technical Meeting, Anaheim, California, U.S.A, pp 433-438.

Rothacher, M., T. A. Springer, S. Schaer, and G. Beutler (1997). "Processing strategies for regional GPS networks", Proceedings of the IAG General Assembley in Rio de Janeriro, Springer Verlag, New York, pp. 93-100.

Saastamoinen, J. (1972). "Atmospheric correction for troposphere and stratosphere in radio ranging satellites", Geophysical monograph, 15, *American Geophysical Union*, Washington, D. C., USA, pp. 247-252.

Schuler T. (2001). "On ground-based GPS tropospheric delay estimation", Ph.D thesis, University of Munchen.

Skone S. (2003). "Atmospheric Effects on GNSS", ENGO633 course, University of Calgary.

Tachikawa, Y., N. B. Nawarathna, B. E. Vieux (2003). "Hydrologic Prediction Using Weather Radar Information and Distributed Hydrological Modeling", The XXIII General Assembly of the International Union of Geodesy and Geophysics, Sapporo, Japan.

Thayer, G. D. (1974). "An improved equation for the radio refractive index of air", *Radio Science*, Vol.9, No.10, pp. 803-807.

Zhang, Y. and C. Bartone (2006). "Single-site carrier phase based troposphere integrity monitoring", Proceedings of ION National Technical Meeting, San Diego, California, U.S.A, pp. 530-542.